

## Sub-nanometer resolution of atomic motion during electronic excitation in phase-change materials

Optical recording materials such as those used for DVD-RAM are semiconducting chalcogen compounds largely composed of Te and the class of such compounds is often referred to as phase-change materials (PCMs). To date, the typical time for phase change between the amorphous and crystalline states has been thought to be on the order of a nanosecond. In recent years, however, first-principles calculations have predicted that by use of electronic excitation, such transitions can be made to occur on picosecond time scales. If these predictions are realized, both low power operation and high data throughput of phase-change memory will be possible.

By intentionally creating an excited state in a solid, it is possible to induce displacements in atomic positions allowing manipulation of the crystal structure of the solid [1]. The displacements of atomic positions in an excited state, however, occur typically on sub-nanometer length scales making it impossible to detect such small changes using visible laser light with a wavelength of several hundred nanometers. In order to measure such small changes in atomic position on picosecond time scales, it is necessary to use sub-nanometer wavelength light from an X-ray laser in a measurement such as time-resolved X-ray diffraction (XRD). We have used the free-electron X-ray laser facility, SACLA BL3, to carry out time-resolved XRD measurements of the atomic motion in an optically excited phase-change material [2].

In the experiment, epitaxial  $\text{Ge}_2\text{Sb}_2\text{Te}_5$  films (thickness 35 nm) grown on a silicon substrate were excited with ultrashort laser light (30 fs, 800 nm). In order to capture the resulting atomic motion after excitation, XFEL pulses (10 fs, 10 keV) were used to stroboscopically observe changes in the sample structure using a multiple port readout CCD (MPCCD) detector to record time-resolved XRD images (Fig. 1). The (222) diffraction plane was chosen for observation in the time-resolved diffraction experiments and changes in both the location and intensity of the XRD peaks were observed with sub-picosecond time resolution (Fig. 2). In addition, as the (222) diffraction vector probed atomic displacements normal to the surface, the symmetry of the diffraction geometry was optimal for observing the atomic displacements induced by the pump laser. In this way, the changes in the positions of the atoms constituting the  $\text{Ge}_2\text{Sb}_2\text{Te}_5$  single crystal could be followed on an ultrafast sub-picosecond time scale.

The displacement of atoms was found to reach a

maximum at about 20 ps (Fig. 2(b)) after the laser pump pulse resulting in a maximum diffraction peak shift ( $0.05 \text{ \AA}^{-1}$ ) with a corresponding atomic displacement of about 2 picometers. Subsequently after a few ns, the atom positions were found to revert to their original positions. Shifts to lower angles of the XRD peaks reflect an increase in the lattice spacing of the crystal, while reductions in the intensity of the peaks reflect an increase in the magnitude of mean square vibrations of the atoms around their average positions (Debye-Waller Effect). The changes are schematically indicated in the bottom of Fig. 1, which visualizes the initial lattice softening resulting from bond breaking (frame I) and the following local atomic rearrangements induced by the electronic excitation (frame II). Subsequent to this, electron-phonon interactions induce a rapid rise in the lattice temperature leading to an expansion of the lattice plane spacing (frame III).

As shown in Fig. 3(a) the diffraction peak intensity does not fully recover even 1.8 ns after excitation due to residual thermal effects, which completely disappear after 3~5 ns depending on the excitation fluence. The return of the diffraction peak to its initial intensity level demonstrates that the  $\text{Ge}_2\text{Sb}_2\text{Te}_5$  film is not amorphized by the laser pump pulse and that the pump-probe process is fully reversible. For finer

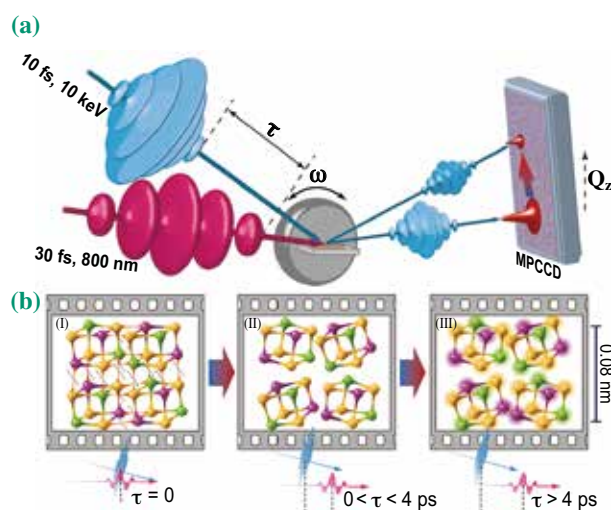


Fig. 1. (a) A schematic representation of the pump-probe time-resolved XRD technique.  $\omega$  represents the rotation of the sample and  $Q_z$  represents the scattering vector. (b) Frames (I) to (III) show schematic changes in the  $\text{Ge}_2\text{Sb}_2\text{Te}_5$  single crystal induced by the femtosecond excitation pulse. Ge atoms are shown in green, Te atoms – in yellow, and Sb atoms are shown in purple.

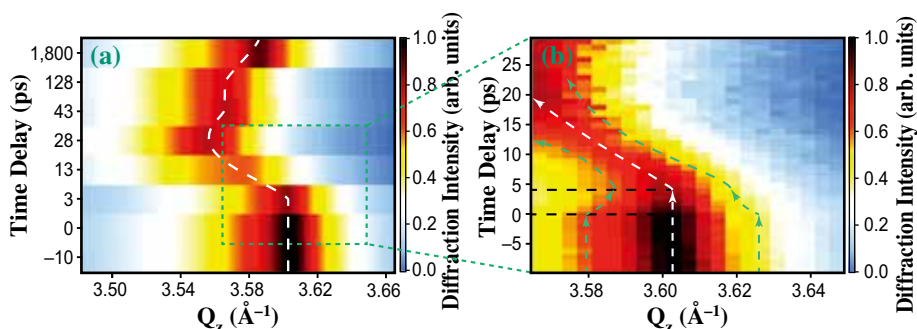


Fig. 2. Time-resolved changes in (222) plane XRD signal. White dashed line indicates the peak position of the signal and green dashed lines show the change of whole diffraction spot. (a) Changes in the XRD peak from  $-10 \sim +1800$  ps (1.8 ns) are shown. The horizontal axis is the scattering vector. (b) Changes in the XRD peak from  $-10 \sim +30$  ps are shown in magnified form.

delay time steps for times up to 10 ps (Fig. 3(b)), we found different dynamics between the diffraction peak intensity and the corresponding peak position shift after excitation that is clearly indicated by an inflection point in the time-dependent diffraction intensity curve and the absence of a diffraction peak position change until 4 ps. These observations indicate the lack of thermal effects immediately after laser exposure.

The current research results suggest that the phase change process in both rewritable optical recording

films and nonvolatile memory phase-change materials can occur on picosecond time scales. Also recently it was found that similar sub-picosecond processes occur in thin film GeTe/Sb<sub>2</sub>Te<sub>3</sub> superlattices [3]. The application of the current techniques to phase change in superlattices may lead to future generations of phase-change material based devices that switch at sub-terahertz rates while offering lower power operation than the current generation of Ge<sub>2</sub>Sb<sub>2</sub>Te<sub>5</sub> polycrystalline films.

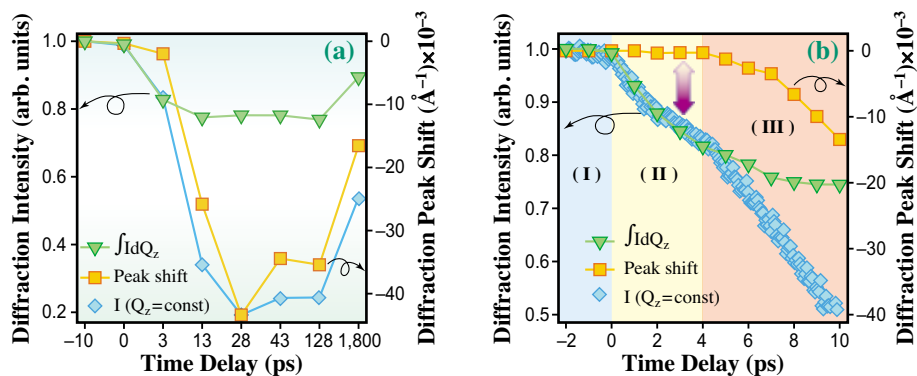


Fig. 3. (a) Normalized integrated diffraction intensity (inverted triangles) and corresponding peak position shift along  $Q_z$  (squares), together with normalized integrated diffraction intensity (diamonds) for a fixed X-ray beam angle of incidence as a function of time up to 1800 ps. (b) The same as (a) but for a finer time delay step up to 10 ps. The both-side arrow indicates the different dynamics between the diffraction integrated intensity and the peak position. The three stages labeled (I), (II), and (III) correspond to the atomic configuration process in Fig. 1.

Kirill V. Mitrofanov<sup>a</sup>, Paul Fons<sup>a</sup> and Muneaki Hase<sup>a,b,\*</sup>

<sup>a</sup> Nanoelectronics Research Institute, National Institute of Advanced Industrial Science and Technology

<sup>b</sup> Division of Applied Physics, Faculty of Pure and Applied Sciences, University of Tsukuba

\*Email: mhase@bk.tsukuba.ac.jp

## References

- [1] A.V. Kolobov *et al.*: Nat. Chem. **3** (2011) 311.
- [2] K. V. Mitrofanov, P. Fons, K. Makino, R. Terashima, T. Shimada, A. V. Kolobov, J. Tominaga, V. Bragaglia, A. Giussani, R. Calarco, H. Riechert, T. Sato, T. Katayama, K. Ogawa, T. Togashi, M. Yabashi, S. Wall, D. Brewé and M. Hase: Sci. Rep. **6** (2016) 20633.
- [3] M. Hase *et al.*: Nat. Commun. **6** (2015) 8367.